CHEMCOMM
Communication
www.rsc.org/chemcomm

Design and post-functionalisation of ordered mesoporous zirconia thin films†

Eduardo L. Crepaldi,[a] Galo J. de A. A. Soler-Illia,[a] David Grosso,[a] Pierre-Antoine Albouy[b] and Clément Sanchez*[a]

[a] *Laboratoire Chimie de la Matière Condensée, Université Pierre et Marie Curie, 4 Place Jussieu, 75252 Paris Cedex 05, France. E-mail: clems@ccr.jussieu.fr.*
[b] *Laboratoire de Physique des Solides, Université Paris-Sud, 91405 Orsay Cedex, France*

Received (in Cambridge, UK) 25th May 2001, Accepted 13th July 2001
First published as an Advance Article on the web 6th August 2001

Bidimensional hexagonal or centred-rectangular mesoporous zirconia thin films have been reproducibly prepared by evaporation-induced self-assembly (EISA), which are stable up to 300 °C, with pore size around 35 Å; the films can be post-functionalised with organic ligands presenting different functions, opening a land of opportunities for the design of new hybrid mesostructured materials, based on the synergy of a transition metal oxide network and organic groups.

Since Beck and coworkers[1] demonstrated the use of arrays of amphiphilic species as 'supramolecular templates', mesoporous materials have been receiving increasing attention.[2,3] However, the hydrothermal treatment usually applied in the synthesis procedures is not adequate for the processing of mesoporous films, fibres or monoliths. The evaporation-induced self-assembly (EISA)[4] process represents an alternative way to design mesostructured organic–inorganic hybrids, which are precursors for mesoporous solids. By this process, silica based mesoporous materials have been prepared as powders, fibres, monoliths and thin films in a variety of structural arrangements (2D- and 3D-hexagonal, cubic and lamellar phases).[1,5] This same process has been applied to obtain transition metal oxide-based materials, such as mesoporous TiO_2,[6] ZrO_2, Nb_2O_5, Al_2O_3, SnO_2, WO_3, Ta_2O_5 and many mixed metal oxides.[7] For these systems, this approach has been applied mainly to the preparation of powders, or even titania mesoporous films.[8]

Here, we report for the first time to the best of our knowledge, the preparation of oriented mesostructured zirconium oxide-based hybrids and mesoporous oxide films. The post-functionalisation of the zirconia mesoporous films is also reported. Zirconia mesoporous films are particularly interesting because of the high chemical stability of this oxide, being potentially applicable as catalyst support, adsorbent, heavy duty membranes and chemical sensors.

Films were prepared by dip-coating glass or silicon substrates at a constant withdrawal speed ranging from 0.08 to 0.4 cm s^{-1} at room temperature (20–23 °C). The dipping solutions contain 1 $ZrCl_4$: 0.05 Brij-58 [$C_{16}H_{33}(CH_2CH_2O)_{20}OH$] : 40 EtOH : 0–20 H_2O.[9] The relative humidity (RH) inside the dip-coater chamber is a parameter of paramount importance, and was thus controlled between 10 and 80%. After drying, the as-prepared films were submitted to a sequence of treatments in order to stabilise the structure and remove the surfactant: drying overnight at low humidity (< 10%), 12 h at 60 °C, ammonia atmosphere (30 min), and calcination in air at temperatures ranging from 150 to 500 °C for 2 h (ramp of 1 °C min^{-1}).

Two-dimensional XRD patterns in transmission mode demonstrate that a hexagonal (*p*6*m*) mesophase is obtained upon dip-coating, the organised domains are mono-oriented, as previously observed in silica and titania mesoporous films.[8,10] Fig. 1(a)–(c) shows representative 2D-XRD patterns of films treated at 60, 220 and 300 °C, respectively. The observed spots can be indexed in all cases in a 2D-centred-rectangular cell

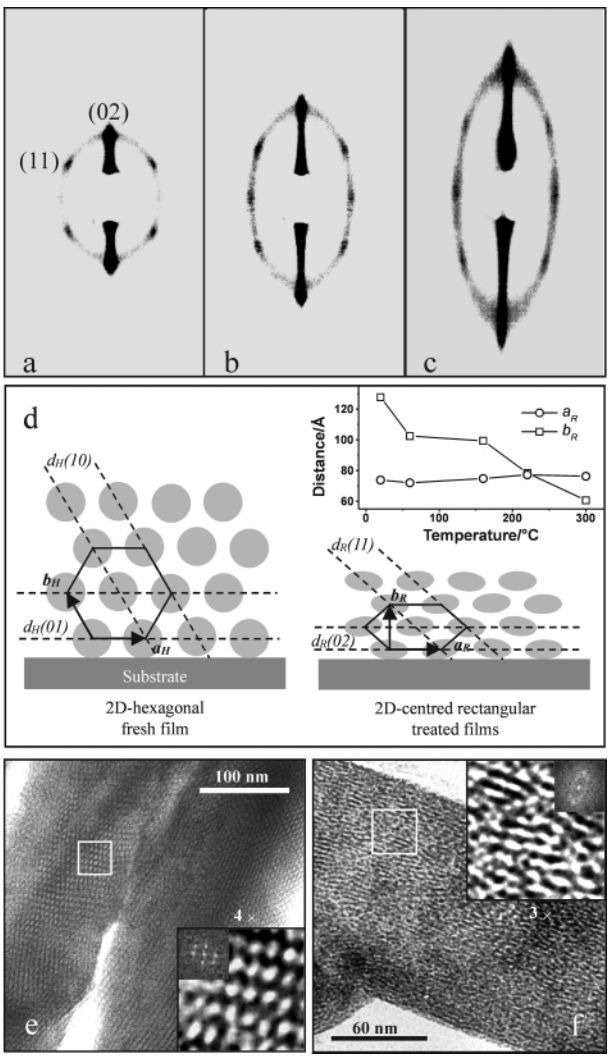

Fig. 1 Two-dimensional XRD patterns obtained by transmission for films treated at (a) 60, (b) 220 and (c) 300 °C. Schematic representation of the relationship between 2D-hexagonal (*p*6*m*) and 2D-centred rectangular (*c*2*m*) cells (d), the inset showing the observed variation of the parameters a_R and b_R of the 2D-centred rectangular cell with temperature. TEM images along the [001] zone axis of Brij 58-templated mesostructured zirconia films treated at (e) 60, and (f) 300 °C. Inset in parts (e) and (f) are reconstructed images and moduli of the Fourier transform of the indicated regions.

† Electronic supplementary information (ESI) available: XRD and SEM data showing the influence of water content in solution and atmospheric relative humidity in the organisation and optical quality of the films, and details about the post-functionalisation. See http://www.rsc.org/suppdata/cc/b1/b104623n/

 DOI: 10.1039/b104623n

(space group *c*2*m*), resulting from a preferential contraction of the hexagonal mesophase in the direction normal to the substrate.[8,10] Low-angle XRD analysis in θ–2θ mode (graphite-monochromated Cu-Kα_1 radiation, λ = 1.5406 Å) of the as-prepared films only showed the presence of a single peak at d = 63.9 Å, corresponding to the d_{02} spot of the bidimensional rectangular (*c*2*m*) lattice [equivalent to the d_{01} distance of the hexagonal (*p*6*m*) structure, see Fig. 1(d)]. The uniaxial contraction in the direction normal to the substrate upon thermal treatment is clearly observed by θ–2θ and 2D-XRD [see inset in Fig. 1(d)], the a_R parameter remaining almost constant (*ca*. 76 Å).

TEM images of films (detached from the substrate, embedded in epoxy resin and ultramicrotomed) support the XRD data, showing almost circular pores for films treated between 60 and 160 °C, and elliptical pores for films treated between 200 and 300 °C, clearly a consequence of the uniaxial contraction. Representative examples are shown in Fig. 1(e) and 1(f). Moreover, images obtained for films treated at low temperatures (60–160 °C) display regular long-range ordered patterns, in accord with XRD data that showed narrow, intense diffraction peaks (or spots, in the 2D-XRD pattern). The partial degradation of the structure can be clearly visualised from Fig. 1(e), that shows broad diffractions for films treated at temperatures > 200 °C, and the presence of an ellipse (characteristic of entangled worm-like channels[10]), the intensity of which increases with temperature. The wall thickness was estimated from TEM to be *ca*. 37 Å for the film treated at 60 °C, decreasing to *ca*. 20 Å upon treatment at 300 °C, probably as a consequence of further condensation, as showed by TGA–DSC analysis. The pore diameter was estimated to be *ca*. 35 Å for films treated between 60 and 160 °C; thermal treatment at 300 °C results in *ca*. 14 × 36 Å pores. N_2 adsorption data (scratched films treated at 220 °C followed by UV/O_3 treatment) showed an average pore diameter of 28 Å (BJH) and specific surface (BET) of 192 $m^2\ g^{-1}$.

Films were prepared in different conditions by varying the water contents in the solution ($h = H_2O/Zr = 0$–20) and the relative humidity (RH 10–80%) (ESI†). In general, 'dry' conditions (low h and RH) lead to non-organised coatings, confirming the essential role of water in solution and evaporation rate.[6] The organisation increases for higher h values, and in most cases, with increasing relative humidity. However, the highest degree of organisation was observed with h = 20 and 10% RH. This result confirms the importance of the evaporation rate, relatively fast (drying within 1 min) at 10% RH and very slow at high humidity conditions.

Despite the high degree of organisation attained for high water contents, the optical quality of the coatings is poor, due to a phase segregation (observed by SEM) (ESI†). In order to obtain transparent films, a two-step process was developed. Submitting fresh films (h = 20; RH% = 10) to a high humidity atmosphere (RH > 80%) for a short time (5–10 s) resulted in the incorporation of water. A second drying process led to transparent and homogeneous films. A SEM image of a film submitted to this treatment shows a completely smooth surface, and the corresponding XRD diagram presents a narrow, intense peak with a *d*-spacing of 63.9 Å. These results indicate that the as-prepared films are quasi-liquid, showing a liquid crystal behaviour, as shown before by Brinker *et al.* for silica films.[4,11] The post-processing (submission to high humidity for few seconds) facilitates homogeneous texture, and leads to better organised domains in the mesostructure, indicated by the narrowing and increasing in intensity of the XRD peak. The thickness of such films as estimated by SEM was 700 nm, and can be tailored by varying the withdrawal speed and the ethanol content in the solution without any noticeable variation in the structure or optical quality.

Following drying overnight at low humidity and room temperature, the *d*-spacing slightly contracted from 63.9 to 63.0 Å while subsequent ammonia vapour treatment resulted in a *d*-spacing of 57.3 Å, indicating further condensation of the zirconium oxide network. From this point on, the films were submitted to thermal treatment, in order to increase the stability of the inorganic network and to remove the surfactant. TGA–DSC analysis of detached films (1 °C min^{-1}, air flow) shows that surfactant decomposition occurs from 150 to 350 °C (26.5 mass%). A crossed XRD-FTIR analysis showed that contraction is small [$(d_0 - d)/d_0 < 22\%$] up to 200 °C; in this range, the surfactant is not removed. From 200 °C on, a strong contraction was observed (40–52% in the range 200–300 °C) coinciding with the decomposition of the surfactant. By 350 °C the mesostructure is lost. However, organic or carboxylate species (detected by FT-IR bands at *ca*. 1618 and 1378 cm^{-1}) cannot be removed, even at 400 °C. An alternative combination of UV light and ozone at room temperature was thus performed,[12] giving rise to pure zirconia mesoporous films.

In order to tailor the nature of the pore surfaces, organic molecules were grafted on the mesoporous zirconia films. Three grafting functions were selected, known by their ability of complexing Zr(IV): β-diketonate, carboxylate and phosphonate. The probe molecules were chosen because of their different properties: dibenzoylmethane, (DBM) and phenylphosphonic acid, (PPA) carrying hydrophobic groups, can be used to impart hydrophobic properties to the pore surface. Methyl red dye, (MTR) is well known as a pH indicator. Finally, ferrocenecarboxylic acid (FCA), is interesting due to its redox properties. FT-IR and UV–VIS data clearly show the grafting of the probes (ESI†). The possibility of ready post-functionalisation of the film, leading to pores with a tailored surface, is a very interesting result, since functionalised films can be applied in many fields, depending on the nature of the grafted species.

Financial support from the French Ministry of Research, CNRS, CNPq (Brazil, grant # 200635/00-0), CONICET and Fundación Antorchas (Argentine Republic) is gratefully acknowledged.

Notes and references

1 C. T. Kresge, M. E. Leonowicz, W. J. Roth, J. C. Vartuli and J. S. Beck, *Nature*, 1992, **359**, 710; J. S. Beck, J. C. Vartuli, W. J. Roth, M. E. Leonowicz, C. T. Kresge, K. D. Schmitt, C. T.-W. Chu, D. H. Olson, E. W. Sheppard, S. B. McCullen, J. B. Higgins and J. L. Schlenker, *J. Am. Chem. Soc.*, 1992, **114**, 10834.
2 C. Göltner and M. Antonietti, *Adv. Mater.*, 1997, **9**, 431.
3 S. Mann, S. L. Burkett, S. A. Davis, C. E. Fowler, N. H. Mendelson, S. D. Sims, D. Walsh and N. T. Whilton, *Chem. Mater.*, 1997, **9**, 2300.
4 C. J. Brinker, Y. Lu, A. Sellinger and H. Fan, *Adv. Mater.*, 1999, **11**, 579.
5 N. K. Raman, M. T. Anderson and C. J. Brinker, *Chem. Mater.*, 1996, **8**, 1682; H. Yang, N. Coombs, I. Sokolov and G. A. Ozin, *Nature*, 1996, **381**, 589; H. Yang, A. Kuperman, N. Coombs, S. Mamicheafara and G. A. Ozin, *Nature*, 1996, **379**, 703; D. Zhao, Q. Huo, J. Feng, B. F. Chmelka and G. D. Stucky, *J. Am. Chem. Soc.*, 1998, **120**, 6024; P. J. Bruinsma, A. Y. Kim, J. Liu and S. Baskaran, *Chem. Mater.*, 1997, **9**, 2507; N. Melosh, P. Lipic, F. S. Bates, F. Wudl, G. D. Stucky, G. H. Frederickson and B. F. Chmelka, *Macromolecules*, 1999, **32**, 4332; D. Zhao, P. Yang, N. Melosh, J. Feng, B. F. Chmelka and G. D. Stucky, *Adv. Mater.*, 1998, **10**, 1380; D. Grosso, A. R. Balkenende, P.-A. Albouy, M. Lavergne, L. Mazerolles and F. Babonneau, *J. Mater. Chem.*, 2000, **10**, 2085.
6 G. J. A. A. Soler-Illia, E. Scolan, A. Louis, P. A. Albouy and C. Sanchez, *New J. Chem.*, 2001, **25**, 156.
7 (*a*) P. Yang, D. Zhao, D. I. Margolese, B. F. Chmelka and G. D. Stucky, *Nature*, 1998, **395**, 583; (*b*) P. Yang, D. Zhao, D. I. Margolese, B. F. Chmelka and G. D. Stucky, *Chem. Mater.*, 1999, **11**, 2813.
8 D. Grosso, G. J. de A. A. Soler-Illia, F. Babonneau, C. Sanchez, P.-A. Albouy, A. Brunet-Bruneau and A. R. Balkenende, *Adv. Mater.*, 2001, **13**, 1085.
9 Care must be taken during the addition of the anhydrous metal chloride into the surfactant alcoholic solution, since the reaction is exothermic and HCl is released.
10 M. Klotz, P.-A. Albouy, A. Ayral, C. Ménager, D. Grosso, A. Van der Lee, V. Cabuil, F. Babonneau and C. Guizard, *Chem. Mater.*, 2000, **12**, 1721.
11 Y. Lu, R. Ganguli, C. Drewien, M. Anderson, C. Brinker, W. Gong, Y. Guo, H. Soyez, B. Dunn, M. Huang and J. Zink, *Nature*, 1997, **389**, 364.
12 T. Clark Jr., J. D. Ruiz, H. Fan, C. J. Brinker, B. I. Swanson and A. N. Parikh, *Chem. Mater.*, 2000, **12**, 3879.